Palaeogeography, Palaeoclimatology, Palaeoecology 692 (2026) 113780

Contents lists available at ScienceDirect

Palaeogeography, Palaeoclimatology, Palaeoecology

journal homepage: www.elsevier.com/locate/palaeo

Controls on the ichnology of late miocene–pliocene shallow-marine strata during uplift of the Taiwan Orogen: A semi-quantitative approach☆

Shahin E. Dashtgard [a,*], Amy I. Hsieh [b], Romain Vaucher [c], Ludvig Löwemark [d]

[a] Department of Earth Sciences, Simon Fraser University, Burnaby, British Columbia, Canada V5A 1S6
[b] Institute of Earth Sciences (ISTE), University of Lausanne, Géopolis, 1015 Lausanne, Switzerland
[c] College of Science and Engineering, James Cook University, Townsville, Queensland, Australia
[d] Department of Geosciences, National Taiwan University, No 1. Sec. 4 Roosevelt Road, 106 Taipei, Taiwan

ARTICLE INFO

Editor: H Falcon-Lang

Keywords:
Ichnology
Tidal straits
Trace fossil preservation
Bioturbation index
Process ichnology

ABSTRACT

Late Miocene through Pliocene shallow-marine sedimentary strata of the Kueichulin Formation are exposed along the Da'an River, Taiwan, and these strata form part of the fill of the Taiwan Western Foreland Basin (i.e., paleo-Taiwan Strait). The ichnology of these strata reflect the emergence and early evolution of Taiwan. Semi-quantitative characterization of trace fossil assemblages in the Kueichulin Formation are used to resolve the dominant controls on the preserved character of trace fossils. The described strata are divided into three phases – pre-emergent, early emergent and emergent – and these three phases are divided into six stages: pre-emergent-lower, pre-emergent-upper, early emergent, emergent-lower, emergent-middle, and emergent-upper. Throughout the pre-emergent-lower stage, seafloor erosion during storms that propagated across the Pacific Ocean exerted the dominant control on the preservation and character of trace-fossil assemblages resulting in a low preservation of bioturbation, especially of shallow-tier burrows. The formation and emergence of Taiwan (upper pre-emergent through emergent-upper stages) resulted in the island acting as a baffle to large storm waves and this is manifested in the increased preservation of: i) shallow-tier burrows constructed by filter feeders and interface (surface) deposit feeders, ii) bioturbated strata, and iii) diverse and abundant trace fossils. There is a noticeable decrease in the preservation of deep-tier burrows in mudstone-dominated strata deposited during the early emergence of Taiwan. Later, increased and more variable sedimentation / substrate mobility resulted in greater bed-by-bed variability in the degree of bioturbation once the Taiwan Strait began to narrow and tidal currents increased in strength (emergent-lower to emergent-upper stages). During the emergent stages, both seafloor erosion during storms and tidal reworking controlled the preservation and character of trace fossil assemblages. The ichnological analysis employed herein demonstrates the value of a semi-quantitative approach to ichnology. Systematic compilation of qualitative ichnological data can be converted into numerical values, which subsequently, can be used to resolve trends in trace fossils abundances, tiering depths, and ethologies, and these data can be used to assess variable controls on preserved character of ichnological assemblages.

1. Introduction

Ichnological research is fundamental in paleoenvironmental reconstructions because trace fossils record the activity of animals during and/or shortly after sediment deposition. While primary sedimentary structures preserve evidence of depositional processes, trace fossils preserve evidence of ambient environmental conditions. However, the preserved ichnological assemblage is not always an accurate representation of paleoenvironmental conditions because of preservational biases that may result in the removal or reworking of sediments colonized by infauna. Additionally, qualitative assessments of ichnological characteristics may mask ichnological responses to a range of autogenic and allogenic forcings. The Upper Miocene to Pliocene Kueichulin Formation comprises mainly shallow-marine sedimentary strata, and here we assess trace fossil assemblages through the Kueichulin Formation. We identify ichnogenera and the degree of bioturbation on a bed-by-bed basis. The abundances of each ichnogenera and bioturbation intensities are quantified and are then used to discuss the linkage between trace

☆ This article is part of a Special issue entitled: 'Ichnology' published in Palaeogeography, Palaeoclimatology, Palaeoecology.

* Corresponding author.
E-mail address: sdashtga@sfu.ca (S.E. Dashtgard).

https://doi.org/10.1016/j.palaeo.2026.113780
Received 6 November 2025; Received in revised form 3 March 2026; Accepted 1 April 2026
Available online 2 April 2026

fossil assemblages and evolution of hydraulic and sedimentation conditions in Taiwan's Western Foreland Basin (TWFB).

The TWFB is situated on the western side of Taiwan and extends below the Taiwan Strait (Lin et al., 2003). Recent work on the Kueichulin Formation has constrained the timing of deposition and sediment accumulation rates; and the same studies have revealed evidence of high-energy events and the transition of depositional environments from an open shelf to a confined strait (Dashtgard et al., 2020; Dashtgard et al., 2021; Hsieh et al., 2023a; Hsieh et al., 2023b; Hsieh et al., 2025; Nagel et al., 2014; Nagel et al., 2013). The evolution in depositional conditions recorded through the Kueichulin Formation allows for the comparison of trace-fossil suites to both physical and chemical stresses and to sediment erosion events.

In the shallow-marine realm, abundant food, oxygen, and energetic flow can result in extensive seafloor colonization by diverse groups of infauna (Ayranci et al., 2014; Howard and Frey, 1984; Reineck and Singh, 1980; Seike et al., 2011) and this is reflected in preserved trace-fossil assemblages (MacEachern et al., 2007; Pemberton et al., 1992; Seilacher, 1964, 1967). Sediments deposited in shallow-marine settings can also show limited bioturbation both as a function of physical and chemical stresses in the environment (e.g., Buatois et al., 2005; Dashtgard and Gingras, 2012; La Croix et al., 2022; MacEachern and Bann, 2020) and as a result of sediment reworking during high-energy events (e.g., storms, river floods; Dashtgard et al., 2020; Pemberton and MacEachern, 1997; Vaucher et al., 2023a). Differentiating between trace-fossil suites that show reduced trace density and diversity because of physical and chemical stresses versus those that are reduced because of sediment erosion is not always possible without prior knowledge of paleoenvironments and their evolution.

The identification of trace fossils is inherently qualitative. Trace fossils can appear similar to multiple ichnogenera depending on their two-dimensional expressions in outcrop (Chamberlain, 1978). Identifiable trace-fossil assemblages also vary as a result of the scale of an outcrop (Marenco and Hagadorn, 2019); their relief (Bromley, 1996; Seilacher, 1964), and whether they are exposed in cross section and/or on bedding planes (Shillito and Gougeon, 2024). Attempts to quantify or semi-quantify qualitative observations are numerous but mainly focus on bioturbation intensity (MacEachern et al., 2007; Reineck and Singh, 1980; Taylor and Goldring, 1993) and tiering relationships (Ekdale et al., 2012; Taylor et al., 2003). Several authors have also employed

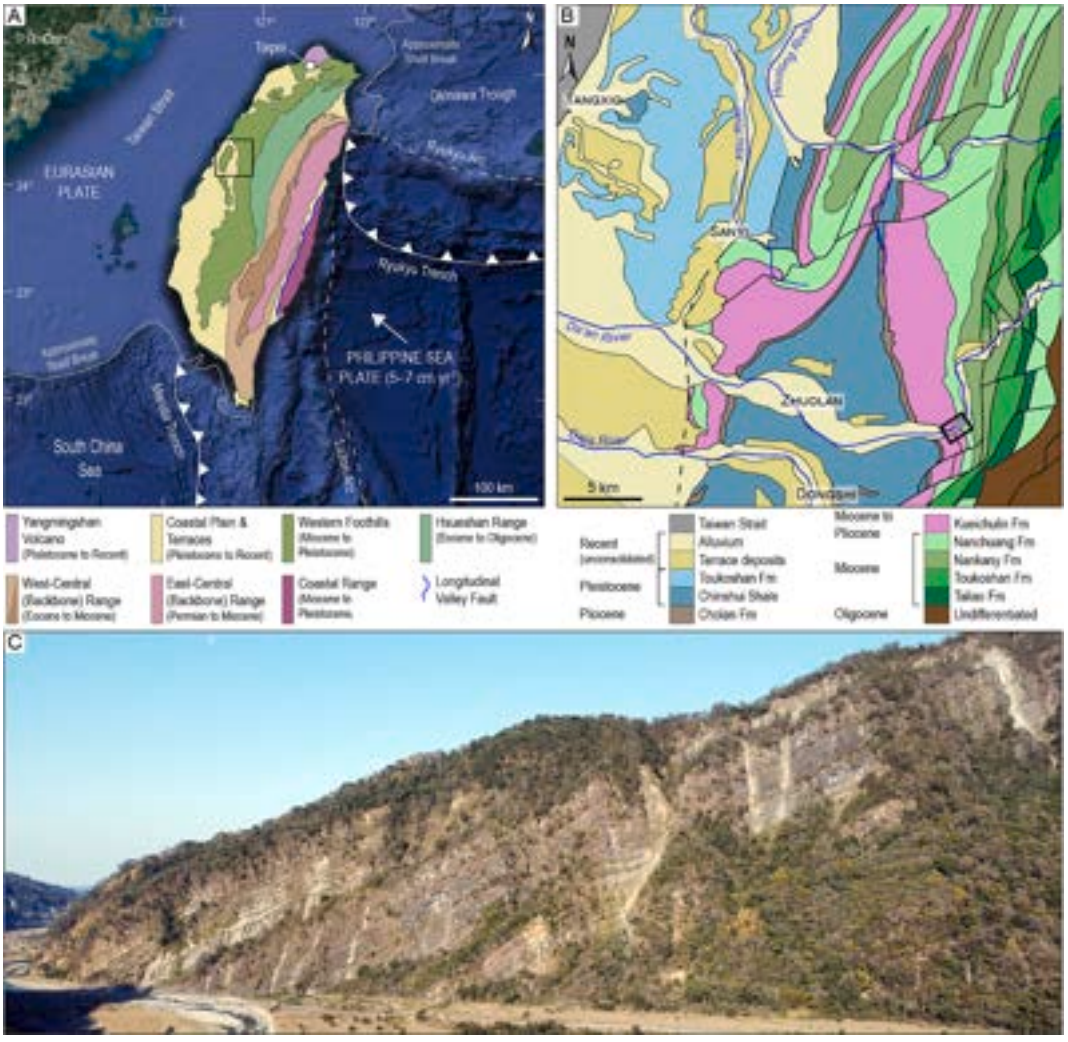

Fig. 1. The study area and studied outcrop. **A)** General geological map of Taiwan showing the major tectonic and geographic elements of and near the island. The black box defines the more detailed geological map depicted in **B**. The present-day rate of relative motion of the Philippine Sea Plate is derived from Lin et al. (2003) and Simoes and Avouac (2006). The general geology of Taiwan is based on Lin and Chen (2016); and the base map is sourced from Google Earth. The legend for the colours used in **A** are shown below the map. **B)** Geological map of west-central Taiwan. The map is derived from MOEA, C.G.S.o.T (2019) and is modified based on formations shown in Lin and Chen (2016) and Teng et al. (1991). The black box defines the position of the outcrop upon which this study is based. The legend for the colours used in **B** are shown below the map. **C)** Photo of part of the Kueichulin Formation outcrop along the Da'an River. The strata get progressively younger to the left.

more quantitative approaches in the analysis of ichnofabrics (e.g., McIlroy, 2007); ichnodiversity (Kikuchi et al., 2018; Singh et al., 2023), movement (Wang and Miguez-Salas, 2025)); and ecosystem engineering (Buatois et al., 2020). Herein, we employ novel methods for advancing semi-quantitative methods in trace fossil analyses.

1.1. Geological background and study area

Taiwan formed through the oblique arc-continent collision of the Philippine Sea Plate and the Eurasian Plate (e.g., Suppe, 1981, 1984). The two plates began colliding in the Late Miocene (~6.5 million years ago (Mya)) and formed the 330 km long; 100 km wide orogenic belt that makes up most of Taiwan (Fig. 1A). The nearly 4000 m high mountain belt continues to uplift at a rate of approximately 5–7 mm per year (Castelltort et al., 2011; Chang et al., 2023; Covey, 1984; Lin and Watts, 2002; Nagel et al., 2018). Through the ongoing collision and over the past 6.5 million years, the main depocenters of the TWFB migrated south-southwestward at a rate of approximately 31.5 km (+10 to −5 km uncertainty) per million years (Shaw, 1996; Simoes and Avouac, 2006), and the continued and persistent uplift of Taiwan has exposed pre-collisional passive margin strata and post-collisional foreland basin strata (Lin et al., 2003; Lin and Watts, 2002; Suppe, 1981, 1984). The TWFB is characterized by both high-accommodation and high-sedimentation rates, with sediment accumulation rates exceeding 400 m per million years in the Early Pliocene, and 1000 m per million years in the late Pleistocene (Chang and Chi, 1983; Chen et al., 2001; Covey, 1984; Simoes and Avouac, 2006; Vaucher et al., 2021; Vaucher et al., 2023b). Upper Miocene to Pliocene sedimentary strata of the Kueichulin Formation were deposited during the early stages of the collision (Lin et al., 2003; Yu and Chou, 2001) and in mainly shallow-marine environments (Castelltort et al., 2011; Covey, 1984; Dashtgard et al., 2020; Dashtgard et al., 2021; Hsieh et al., 2023b; Hsieh et al., 2025; Nagel et al., 2013).

The Kueichulin Formation overlies the Nanchuang Formation and grades both upwards and southwards into the Chinshui Shale (Castelltort et al., 2011). The Kueichulin Formation is up to 800 m thick and consists of three members; including (from base to top): Kuantaoshan Sandstone; Shihliufen Shale; and Yutengping Sandstone (Fig. 2; Castelltort et al., 2011; Lin et al., 2007; Pan et al., 2015; Shaw, 1996). The Kuantaoshan Sandstone records deposition on the eastern margin of the Eurasian Plate between ~6.3 and 5.4 Mya (Hsieh et al., 2023a). The Shihliufen Shale is interpreted as forming near the Miocene-Pliocene boundary and coincides with the collision of the Luzon Arc on the Philippine Sea Plate with the Eurasian Plate starting around 5.4 Mya and continuing to about 4.9 Mya. The Yutengping Sandstone records deposition from 4.9 to 3.2 Mya (Hsieh et al., 2023a).

2. Study area and methods

In this study, we evaluate Late Miocene through Pliocene strata (upper part of the Kuantaoshan Sandstone, Shihliufen Shale and lower part of the Yutengping Sandstone) of the Kueichulin Formation exposed along the Da'an River in the northern extent of the Western Foothills (24.29479° N, 120.91062° E; Figs. 1B and 2). Outcrops were measured and described at the decimeter-scale for their bed thicknesses, lithology, sedimentary structures, and trace fossils. The same outcrops were sampled for geochemical, microfossil, and paleomagnetism analyses (Dashtgard et al., 2020; Dashtgard et al., 2021; Hsieh et al., 2023a; Hsieh et al., 2023b; Hsieh et al., 2025). Facies analysis of most of the strata was completed by Hsieh et al. (2025) and those facies are used herein.

Hsieh et al. (2023c) defines a high-resolution chronostratigraphic model for the Kueichulin Formation that is used to correlate facies to previously defined tectonic events. Dashtgard et al. (2021) and Hsieh et al. (2023b) used geochemical proxies to correlate strata to different stages of Taiwan's uplift (Fig. 3). Facies descriptions of the strata (Table 1; Hsieh et al., 2025) and interpretations of depositional processes (Dashtgard et al., 2020; Nagel et al., 2013) are used to place strata into depositional context and to interpret the dominant hydraulic process(es) that deposited a bed, and the duration that the bed was exposed to colonization by infauna (c.f., Wheatcroft, 1990).

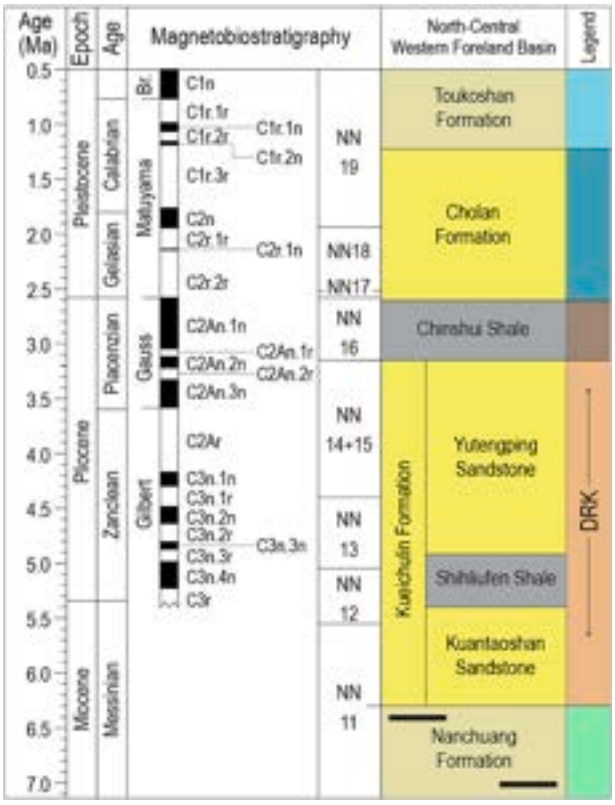

Fig. 2. Chronostratigraphic chart for sedimentary strata in the northern part of the Western Foothills, Western Foreland Basin, Taiwan. Absolute ages, epochs, and ages are based on the International Commission on Stratigraphy chronostratigraphic charts for all of Earth's history (Cohen et al., 2013) and the past 2.7 million years (Cohen and Gibbard, 2016). Formation and member names pertain to the stratigraphy found in the study area (North-Central Western Foreland Basin); and the dominant lithology of those units is indicated by the underlying colours (grayish yellow = terrestrial sandstone; bright yellow = marine sandstone; grey = marine mudstone/shale; and black = coal). The legend and colours in the last column relate to the geological map in Fig. 1B. Nannofossil zonation is based on the International Commission on Stratigraphy; and nannofossil distributions in formations are derived from Horng and Shea (1996) and Pan et al. (2015) and references therein. The chronostratigraphic chart for Taiwan is based on Teng et al. (1991); Lin et al. (2003); Nagel et al. (2013) and Lin and Chen (2016). The magnetobiostratigraphy is from Hsieh et al. (2023c) and references therein. The lithologies of various units are based on this study and MOEA, C.G.S.o.T (2019). Acronyms include: Br (Brunhes, which is a magnetostratigraphic polarity chron) and DRK (Da'an River, Kueichulin Formation). (For interpretation of the references to colour in this figure legend, the reader is referred to the web version of this article.)

The strata described and analyzed in Dashtgard et al. (2020); Dashtgard et al. (2021); Hsieh et al. (2023b); and Hsieh et al. (2025) are used in this study; and are divided into phases that correlate to Taiwan's emergence from the Pacific Ocean. There are three main phases; including pre-emergent; early emergent; and emergent and these are defined based on distinct changes in $\delta^{13}C_{org}$; C/N; magnetic susceptibility; and/or clay mineralogy (Fig. 3; Hsieh et al., 2023b). The pre-emergent phase is further subdivided into pre-emergent–lower and pre-emergent–upper stages based on a distinct change in the preserved ichnological character of strata that define the pre-emergent phase. The early emergent phase is not subdivided and hence is both a phase and a stage. The emergent phase is subdivided into lower, middle, and upper stages based on the preservation of tidal signatures recorded in

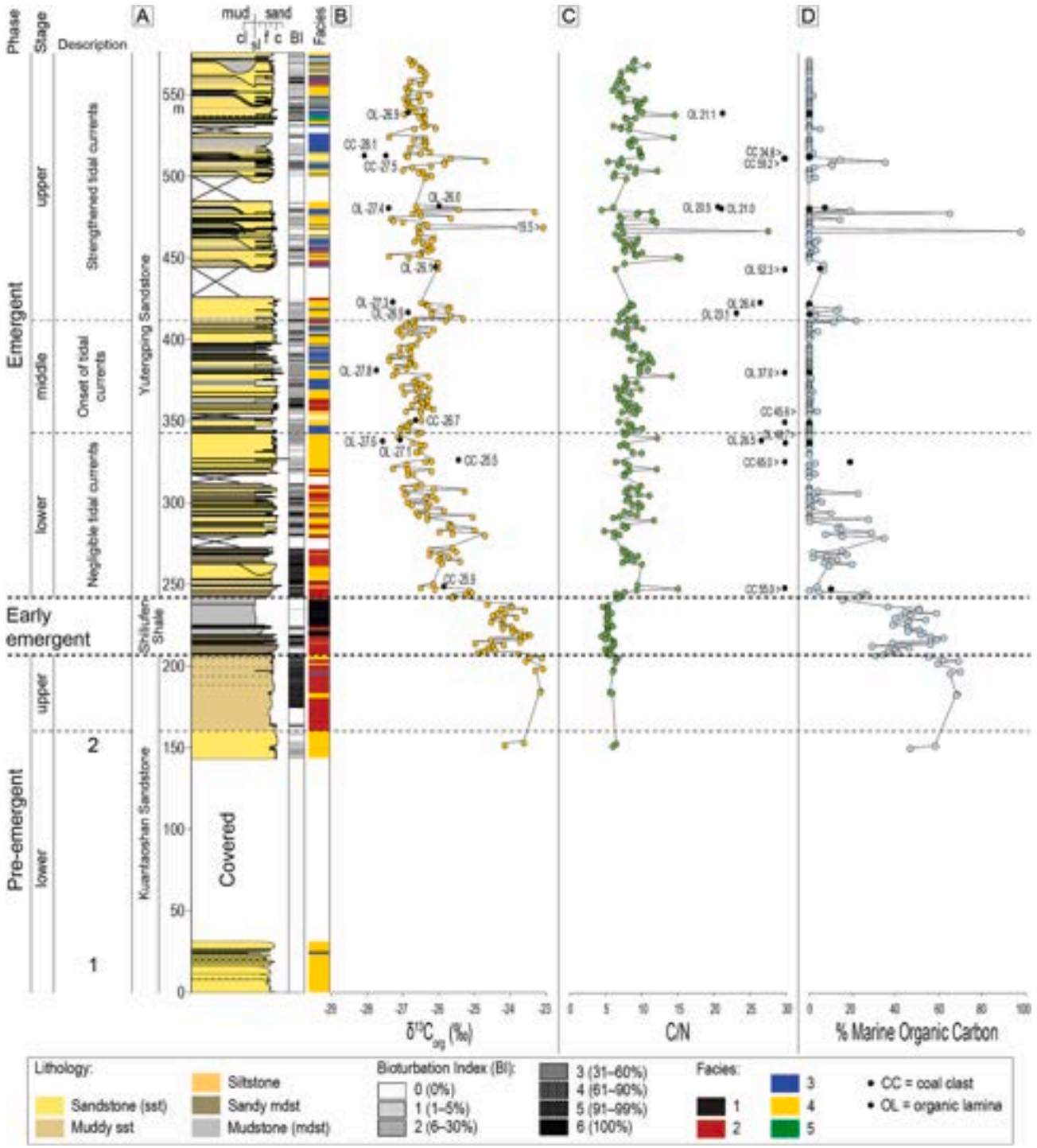

Fig. 3. A) Litholog of the Kueichulin Formation exposed along the Da'an River, Taiwan. The log is derived mainly from Dashtgard et al. (2021) and Hsieh et al. (2023b) with the exception of 0 to 143 m; which is new to this study. The 571 m long section is divided into 3 main phases (pre-emergent; early emergent; and emergent) and 6 stages that are described in the text. In the description column; the labels "1" and "2" refer to the two sections in the pre-emergent–lower stage that are discussed to in the text. All strata are assigned to facies and these are shown in the facies column; facies were assigned mainly by Hsieh et al. (2025) and are presented in Table 1. **B)** Stable carbon isotope values of organic matter ($\delta^{13}C_{org}$). **C)** Carbon:Nitrogen (C/N) ratios. **D)** Calculated percentage of marine-derived organic material for most of the Kueichulin Formation (from Hsieh et al., 2023b).

sedimentary facies. Based on these subdivisions, the six stages defined in this study and their stratigraphic intervals are as follows (Fig. 3): 1) pre-emergent–lower (0–160 m; part of the Kuantaoshan Sandstone); 2) pre-emergent–upper (160–206 m; uppermost Kuantaoshan Sandstone); 3) early emergent (206–239 m; Shihliufen Shale); 4) emergent–lower (239–340 m; lowermost Yutengping Sandstone); 5) emergent–middle (340–407 m; part of the Yutengping Sandstone); and, 6) emergent–upper (407–571 m; part of the Yutengping Sandstone).

Trace fossils are identified to the ichnogenus or ethological group level and are based on two-dimensional expressions in plan view and/or cross-sectional view. Trace fossil occurrences are recorded using AppleCORE® (donated to Simon Fraser University by Mike Ranger) and

Table 1
Table of facies identified in the Kueichulin Formation along the Da'an River (modified after Hsieh et al., 2025)

Facies		Sedimentology		Ichnology	Accessories	Environmental Interpretation
No.	Name	Grain Size	Sedimentary Structures			
F1	Bioturbated MDST	Dominantly mud. Minor vfg sand.	Rare wavy- to planar-parallel laminae of SLST and SST. Coarsening-upward cycles.	BI 3–5. Less commonly 6 and locally 1–2. Traces: Pl, Ro, Sk, Th.	Disarticulated and fragmented shells. Rare coal fragments.	Lower offshore
F2	Bioturbated sandy MDST to muddy SST	Mud with lower vfg to lower fg sand. Locally, lower mg sand.	Rare planar- to wavy parallel-laminated, HCS, or trough cross-bedded SST in MDST. Rare SSD.	BI 4–5. Less commonly 6 and locally 0–2. Traces: Ar, As, Ch, Op, Pa, Ph, Pl, Ps, Ro, Sch, Sk, Te, Th. Rare Di, Sc.	Disarticulated and fragmented shells and *Ditrupa* tubes, MDST rip-up clasts, rare coal fragments.	Upper offshore to distal delta front / prodelta
F3	Interbedded flaser- to lenticular-bedded SST and MDST	Lower vfg to upper fg sand and mud. Up to lower mg sand (locally) in SST beds.	Sharp-based, massive, trough cross-stratified, or parallel-laminated and current-rippled SST with interbedded sharp-based, massive to planar parallel-laminated MDST. Rare SSD.	MDST: BI 1–3. Less commonly 4. SST: BI 0–2. Traces: Ar, As, Ch, Op, Ph, Pl, Ps, Ro, Th. Rare Co, Pa, Sc, Sch, Si.	Rare MDST rip-up clasts. Disarticulated and fragmented shells. Rare coal fragments and carbonaceous laminae.	Delta front in a tidal strait
F4	Massive, planar to trough cross-stratified, and/or hummocky cross-stratified SST	Upper vfg to lower mg sand with interstitial silt and minor clay.	Sharp-based, massive, trough cross- to low-angle planar tabular cross-stratified or amalgamated planar parallel laminated to HCS SST. Wave ripples (locally aggradational) common at top of SST beds. Interbedded organic-rich, structureless to laminated MDST.	BI 0–2, rarely 4–5. Primarily top-down burrows. Traces: Ch, Op (dominant), Pl, Ro, Th. Rare Cy, fu, Ma.	MDST and coal rip-up clasts. Disarticulated and fragmented shells. Abundant carbonaceous laminae.	Wave-dominated delta front to open shelf
F5	Soft-sediment deformed beds	Lower vfg to lower fg sand.	Deformed bedding. Primary stratification not preserved.	BI 0. No primary burrowing preserved.		Post-depositional deformation

Acronyms: Sedimentology: very fine grained (vfg), fine grained (fg), medium grained (mg), Mudstone (MDST), Sandstone (SST), Siltstone (SLST); Sedimentary structures: hummocky cross-stratification (HCS), soft-sediment deformation (SSD) | Ichnology: Bioturbation Index (BI); Trace fossils: *Arenicolites* (Ar), *Asterosoma* (As), *Chondrites* (Ch), *Conichnus* (Co), *Cylindrichnus* (Cy), *Diplocraterion* (Di), fugichnia (fu), *Macaronichnus* (Ma), *Ophiomorpha* (Op), *Palaeophycus* (Pa), *Phycosiphon* (Ph), *Planolites* (Pl), *Piscichnus* (Ps), *Rosselia* (Ro), *Schaubcylindrichnus* (Sch), *Scolicia* (Sc), *Siphonichnus* (Si), *Skolithos* (Sk), *Teichnichnus* (Te), *Thalassinoides* (Th)

are recorded as either individual occurrences or intervals in which they occur regularly. The prevalence of ichnogenera or ethological groups (e.g., fugichnia, navichnia) in each stratigraphic stage is recorded as abundant, common, uncommon, rare, or absent based on their percent coverage within each stage (Table 2). The percent coverage is calcuated by dividing the total thickness of strata in which a trace fossil occurs (in each stage) by the total thickness of strata in the stage. All values are calculated from the AppleCORE log after it was exported in ASCII format. If a trace fossil is recorded as a single occurrence in AppleCORE (i.e., recorded as a point), it is assigned a vertical coverage of 5 cm. Twenty-two ichnogenera or ichnogroups are identified, and the abundance of each trace fossil within each stage is converted to a numerical value using a scale of 0 to 4: absent (0), rare (1), uncommon (2), common (3), and abundant (4; Table 3).

Trace fossils are categorized as shallow tier (confined to the upper 12 cm of sediment; Zhang et al., 2017) or deep tier (extend below 12 cm; Table 3). The number of shallow tier and deep tier trace fossils in a stratigraphic interval is simply the sum of trace fossils that occur in an interval and that are either shallow tier or deep tier. Some trace fossils are both, and hence, are assigned a value of 0.5 in both categories (Table 3). For example, *Chondrites* is exclusively a deep-tier trace fossil and so the presence of *Chondrites* in the emergent-upper zone adds 1 to the sum of deep tier trace fossils in that stage. *Conichnus* is present in the early emergent, emergent-lower, and emergent-middle stages, but *Conichnus* can be both shallow and deep tier. Consequently, 0.5 is added to the sum of both shallow- and deep-tier trace fossils present in the early emergent, emergent-lower, and emergent-middle stages (Table 4). The shallow-tier to deep-tier ratio (S:D) in Table 4 is calculated by dividing the sum of shallow-tier trace fossils by the sum of deep-tier trace fossils.

Table 2
Semi-quantification of trace-fossil abundances recorded in outcrops and based on descriptions recorded in AppleCORE.

Abundance	% Coverage Range	Description
Absent	0	Not observed
Rare	>0 – ≤0.1	Trace present but barely detectable
Uncommon	>0.1 – ≤1	Present, but not common
Common	>1 – ≤10	Frequently observed
Abundant	>10	Dominates visual field / rock surface

Trace fossils are also assigned to ethologies using the classification in Table 1 of Gingras et al. (2007) (Table 3). The categories proposed in Gingras et al. (2007) are simplified into four groups based on feeding modes and/or behaviours; including: filter feeding; deposit feeding; interface feeding; and other. Filter (suspension) feeding is a single category. Deposit feeding includes stoping/mining; and both shallow and deep deposit feeding. Interface (surface deposit) feeding also includes carnivory/scavenging and grazing. "Other" includes escape; equilibrichnia; and locomotion behaviours. Dwellings (living) are not considered because the behaviour is associated with multiple groups (e.g.; many burrows associated with filter feeding; deposit feeding and interface feeding also serve as dwellings) and so this category would closely mimic the sum of the other groups. Waste stowage is also not considered because it is associated with only a few trace fossils and is not listed as the primary function of any of them. Gingras et al.'s (2007) "very strongly associated behaviour" is assigned a value of 3, "commonly associate behaviour" is assigned a value of 2, and "rarely associated behaviour" is assigned a value of 1. The dominance of each feeding behaviour recorded by trace fossils in each stage is calculated using Eq. 1:

$$\sum_{i=1}^{n} B \bullet A \tag{1}$$

Where, B is the value assigned to a behaviour based on how strongly associated it is with a trace fossil (0–3), A is the abundance of the trace fossil in a stratigraphic interval (0–4), and n is the number of trace fossils that reflect that behaviour. For example, Gingras et al. (2007) lists *Arenicolites* twice and indicates this trace fossil is strongly associated with filter feeding (B = 3 for filter feeding), rarely or strongly associated with carnivory / scavenging (B = 3 for interface feeding), commonly associated with interface feeding (B = 2 for interface feeding), commonly to strongly associated with stoping / mining (B = 3 for deposit feeding), and commonly associated with shallow deposit feeding

Table 3
Summary of the trace fossils identified in the three phases and six stages defined for the Kueichulin Formation (Fig. 3). The relative abundance of each trace fossil is shown. Each trace fossil is also classified as shallow tier (confined to the upper 12 cm of sediment) or deep tier (extends below the upper 12 cm). The last four columns show the behaviours represented by each trace fossil as defined in Gingras et al. (2007).

Ichnogenera	Pre-emergent –lower	Pre-emergent –upper	Early emergent	Emergent –lower	Emergent –middle	Emergent –upper	Shallow or Deep Tier		Ethologies from Gingras et al. (2007)			
							Shallow	Deep	Filter feeding	Interface feeding	Deposit feeding	Other
Arenicolites												
Asterosoma												
Chondrites												
Conichnus												
Cylindrichnus												
Diplocraterion												
fugichnia												
Helminthopsis												
Macaronichnus												
navichnia												
Ophiomorpha												
Palaeophycus												
Phycosiphon												
Pischichnus												
Planolites												
Rosselia												
Schaubcylindrichnus												
Scolicia												
Siphonichnus												
Skolithos												
Teichichnus												
Thalassinoides												
Total ichnogenera	3	9	12	16	16	12						

Rare (1) Uncommon (2) Common (3) Abundant (4) Both (0.5) Yes (1) Rare assoc. (1) Common assoc. (2) Very strong assoc. (3)

Table 4
Semi-quantified ichnological data derived from trace fossil assemblages (Table 3). See Methods for an explanation of how these values are derived. Boxes are colour coded to enable comparison. In the Stage total column: ≥200 (dark green), 150–200 (light green), and 100–150 (yellow green). In the S:D ratio column: ≥3 (dark green), 2–<3 (light green), and 1–<2 (yellow green).

	Filter feeding	Interface feeding	Deposit feeding	Other	*Stage Total*	Shallow Tier	Deep Tier	*S:D ratio*
Pre-emergent–lower	10	0	27	4	*41*	2	7	*0.3*
Pre-emergent–upper	37	23	43	29	*132*	16.5	9.5	*1.7*
Early emergent	43	50	39	43	*175*	28.5	6.5	*4.4*
Emergent–lower	59	55	69	38	*221*	29.5	13.5	*2.2*
Emergent–middle	53	63	67	31	*214*	29.5	13.5	*2.2*
Emergent–upper	48	31	70	32	*181*	21	14	*1.5*
Behaviour Total	*250*	*222*	*315*	*177*				

(B = 2 for deposit feeding). The highest B values in each category (filter feeding, interface feeding, deposit feeding, other) are used, and so *Arenicolites* is assigned a 3 for filter feeding, interface deposit feeding and deposit feeding. Since *Arenicolites* occurs uncommonly in the emergent–lower stage, it adds 3 (3·1) to the filter feeding, interface deposit feeding, and deposit feeding categories in that stage.

The degree of bioturbation at the bed scale was recorded in AppleCORE using the bioturbation index (BI; Taylor and Goldring, 1993). Recorded BI values are then used to determine the net thickness of strata (as a percentage) in each stage that preserves that degree of bioturbation

Table 5
Summary of the cumulative thickness of strata (as a percentage of all strata in the stage) that preserves different Bioturbation Index (BI) categories. Boxes are colour coded to enable comparison: ≥ 50% (dark green), 20 – <50% (light green), and ≥ 10% – <20% (yellow green).

Stage	Cumulative thickness of strata displaying each BI category (%)						
	0 (0%)	1 (1–5%)	2 (6–30%)	3 (31–60%)	4 (61–90%)	5 (91–99%)	6 (100%)
Pre-emergent-lower	73	19	7	0	0	0	0
Pre-emergent-upper	0	6	0	4	17	66	8
Early emergent	2	17	11	19	17	19	14
Emergent-lower	12	16	10	5	7	39	11
Emergent-middle	34	23	15	8	6	9	5
Emergent-upper	12	44	16	12	11	6	0

(Table 5). The percentages are calculated from the ASCII file exported from AppleCORE. For example, in the pre-emergent-lower stage, 73% percent of all strata preserve no bioturbation, 19% preserve BI 1, and 7% preserve BI 2; the remaining 1% is lost in rounding errors.

3. Results

The distribution of facies along the logged section is shown in Fig. 3A. In general, facies record deposition on the shelf or in shallower water and probably at less than 50 m water depth (Table 1; Dashtgard et al., 2021; Hsieh et al., 2023b; Nagel et al., 2013). Below are detailed descriptions of the preserved ichnological characteristics in each stage. The ichnological characteristics of each stage are summarized in Table 3. Semi-quantified ichnological data derived from trace fossil assemblages are summarized in Table 4. The prevalence of bioturbation in each stage as recorded by the BI is summarized in Table 5.

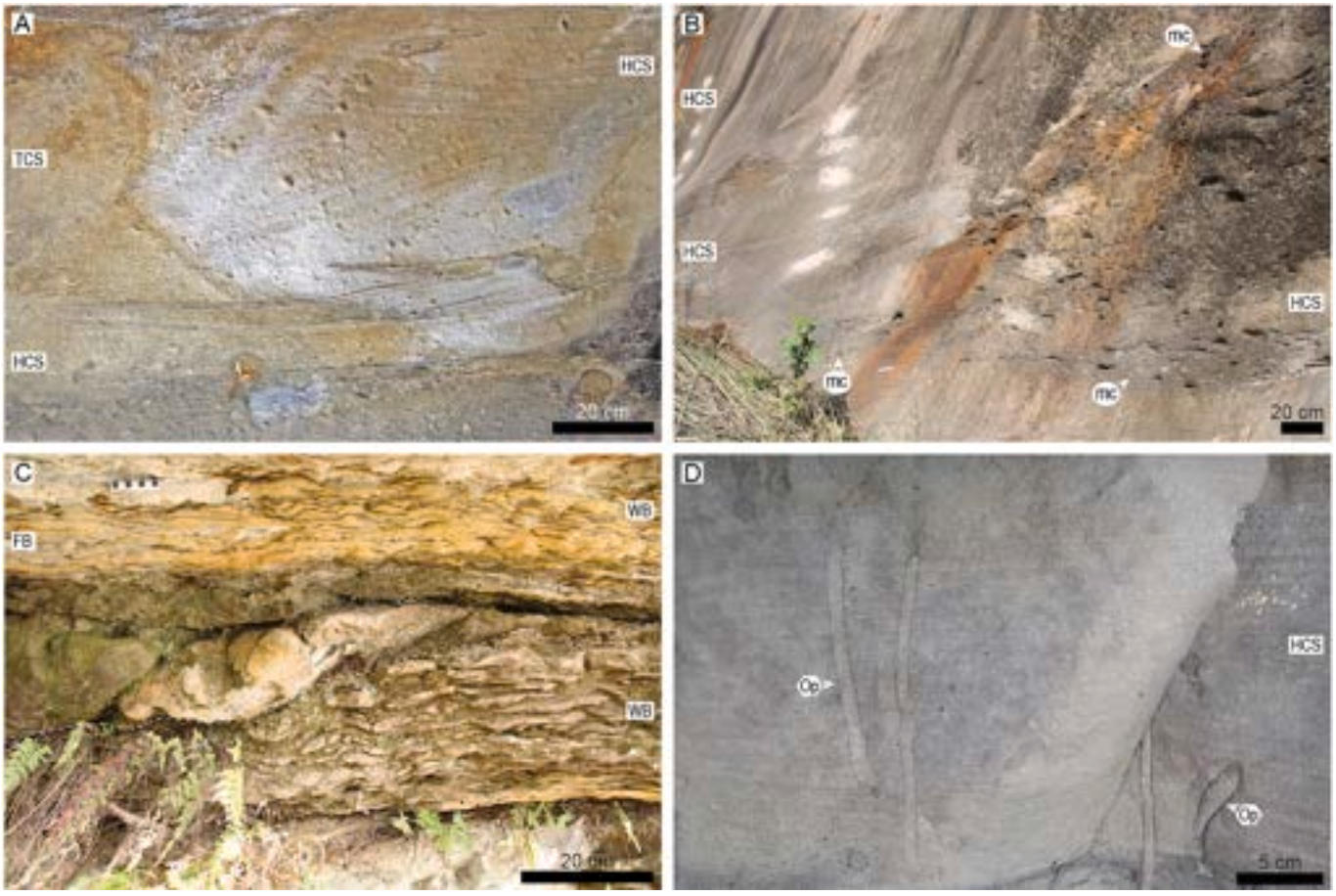

Fig. 4. Photos of the pre-emergent–lower stage (0–160 m) which comprises two sections of exposed strata (1: 0–33 m and 2: 143–160 m, Fig. 3). Square backgrounds for labels indicate sedimentary structures, hexagons indicate trace fossils, and circles indicate accessories (e.g., carbonaceous material, mud clasts). All photos are shown in cross-section view. **A)** Amalgamated trough cross stratification (TCS) and hummocky to swaley cross-stratification (HCS) in sandstone (Facies 4; 5–10 m). The thin dashed white lines mark scour surfaces between sedimentary structures. **B)** Beds of mud-clast (mc) breccia that are both interbedded and grade laterally into hummocky cross-stratified sandstone (Facies 4; 5–10 m). **C)** Wavy-bedded (WB) to flaser-bedded (FB) heterolithics (Facies 3). Note the small channel with the scoured lower surface (dashed white line; 26.3–27.9 m). **D)** Vertical shafts of *Ophiomorpha* in hummocky cross-stratified sandstone with BI 1 (Facies 4; 149–150 m).

3.1. Pre-emergent phase (0–206 m)

The pre-emergent phase comprises two distinct stages that are distinguished based on their sedimentological and ichnological character; these are referred to as lower (0–160 m) and upper (160–206 m; Fig. 3). The pre-emergent–lower stage comprises two outcrop sections (1 and 2) separated by a 110 m long covered interval (Fig. 3). Section 1 is approximately 33 m thick and comprises mainly Facies 4 (Fig. 4A–B) with uncommon preservation of Facies 3 (Fig. 4C). Section 2 is approximately 17 m thick and comprises mainly Facies 4 (Fig. 4D).

Three ichnogenera are observed in the pre-emergent–lower stage, including abundant *Ophiomorpha* (Fig. 4E–F), common *Thalassinoides*, and uncommon *Planolites* (Table 3). The degree of bioturbation is the lowest of all stages with >90% of strata preserving BI 0 or 1 (Table 4). The pre-emergent-lower strata preserve more than 3 times as many deep-tier trace fossils to shallow-tier ones (S:D = 0.3; Table 5). The most commonly observed trace fossils are associated with deposit feeding.

The pre-emergent–upper stage records mainly Facies 2 (Fig. 5A, C–D) with lesser Facies 4. Interbedded Facies 3 is rarely preserved (Fig. 5B). The preserved trace fossil suite in the pre-emergent-upper stage comprises 9 ichnogenera/ethological groups, including: abundant *Ophiomorpha* and *Rosselia*; common *Planolites*, *Schaubcylindrichnus*, *Skolithos*, and *Thalassinoides;* and, uncommon navichnia, *Phycosiphon*, and *Teichichnus* (Table 3). The pre-emergent–upper stage preserves the highest degree of bioturbation of all stages with >90% of beds preserving BI 4–6 (Table 4). The increase in ichnogenera and bioturbation intensity from the pre-emergent-lower stage corresponds to an abrupt shift from mainly deep-tier to mainly shallow-tier trace fossils (S:D = 1.7; Table 5). The most commonly observed trace fossils are associated with deposit feeding and filter feeding, but there is also a substantial increase in the number of traces that record interface feeding and other behaviours.

3.2. Early emergent phase (206–239 m)

The early emergent phase corresponds to the Shihliufen Shale (Figs. 2 and 3), and these strata comprise mainly Facies 1 and 2 (Table 2; Figs. 3 and 6). Bioturbation is highly variable in the early emergent phase: BI 0 is recorded in 2% of all beds, and beds displaying higher degrees of bioturbation (BI categories 1 through 6) are near-equal, comprising 11–19% each (Table 4). Highly bioturbated sections are typically associated with Facies 1 mudstone, but in monolithic mudstone, the lack of sediment contrast masks burrows giving the appearance of BI 0–2 with only sand-filled burrows being evident (Fig. 6B). This low degree of bioturbation is not considered to be an accurate reflection of the degree of burrowing as interbedded sandstone and mudstone or siltstone and mudstone intervals show BI 3–5 (Figs. 3 and 6A). The preserved trace fossil suite comprises 12 ichnogenera/ethological groups, including: abundant *Planolites*, *Rosselia,* and *Thalassinoides*; common navichnia, *Palaeophycus*, *Piscichnus*, *Skolithos*, and

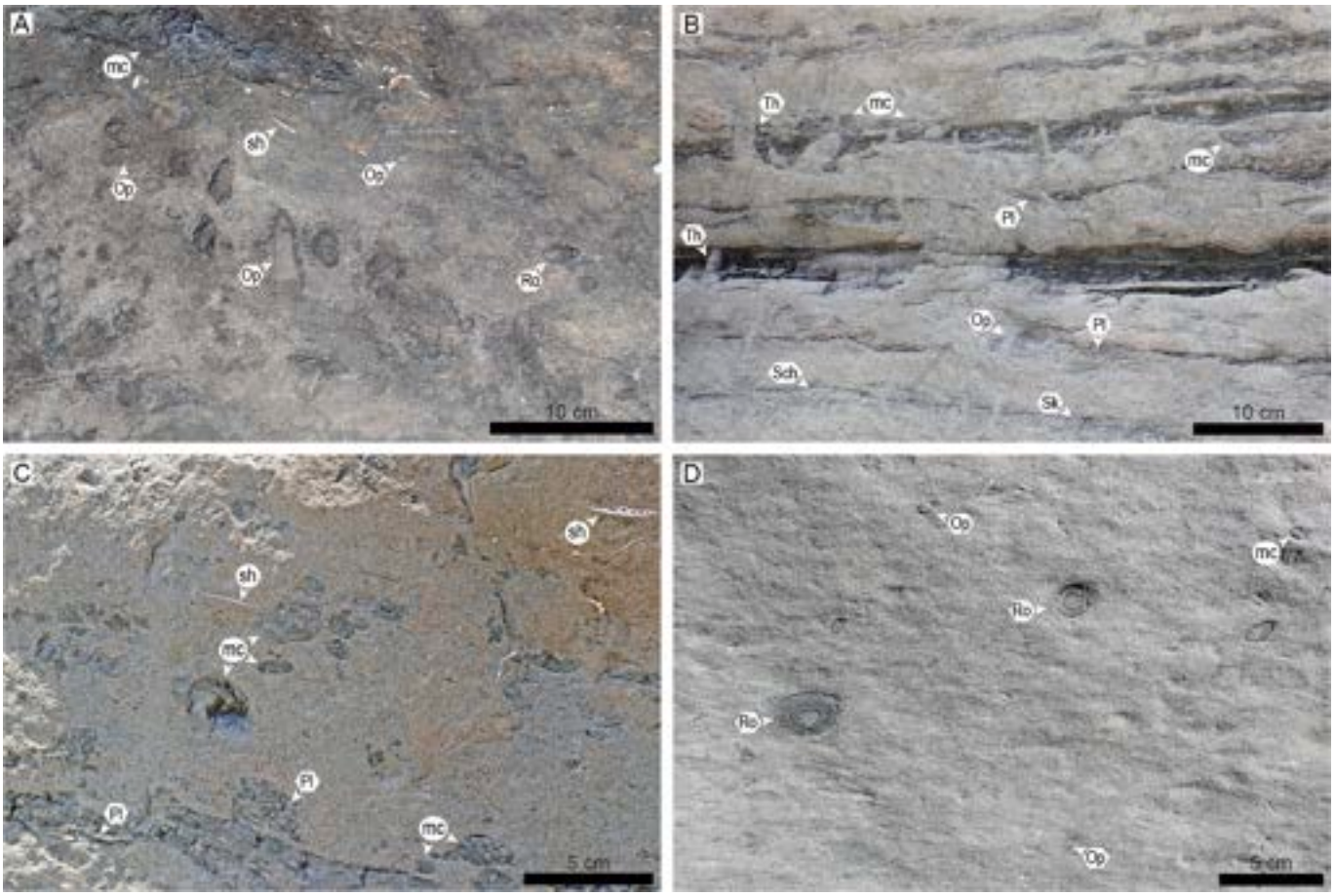

Fig. 5. Photos of the pre-emergent–upper stage (160–206 m). Hexagon backgrounds for labels indicate trace fossils, and circles indicate accessories (e.g., carbonaceous material, mud clasts). **A)** Highly bioturbated (BI 5) muddy sandstone of Facies 2 with mud clasts (mc) and shell fragments (sh) (oblique view, 182–183 m). **B)** Interbedded medium-grained sandstone and mudstone (Facies 3) that shows BI 2–4 (cross-section view, 196–197 m). **C)** Seemingly structureless (bioturbated?) medium-grained sandstone (Facies 2?) with mud clasts and shell fragments. Note the concentration of *Planolites* in the mud clasts (cross-section view, 196–197 m). **D)** Probably completely bioturbated sandstone (BI 6, Facies 2) with *Ophiomorpha* and *Rosselia* burrows (plan view, 199 m). Trace fossil acronyms: *Ophiomorpha* (Op), *Planolites* (Pl), *Rosselia* (Ro), *Schaubcylindrichnus* (Sch), and *Skolithos* (Sk).

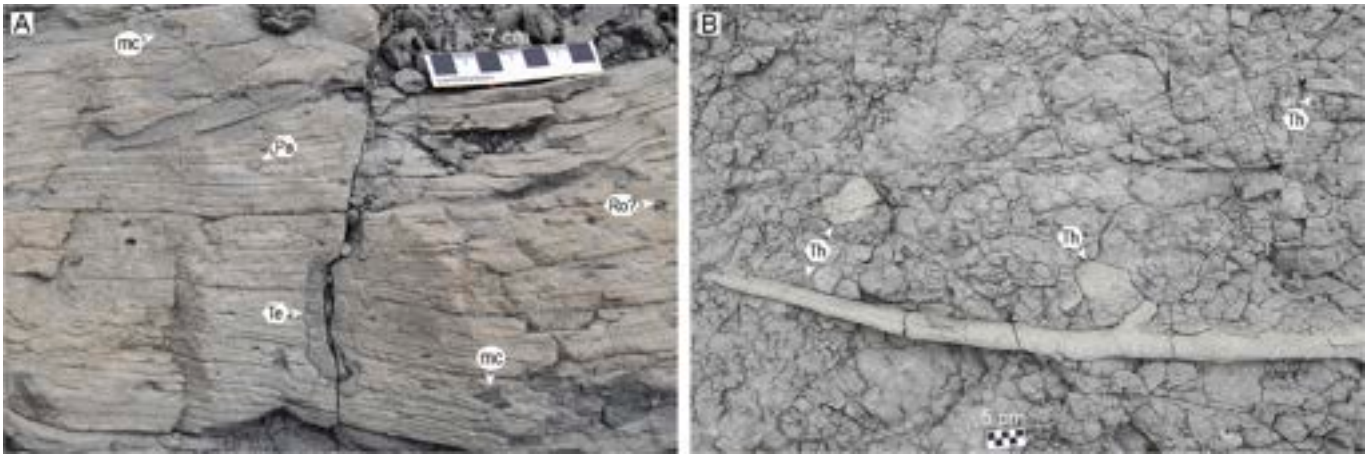

Fig. 6. Photos of the early emergent stage (206–239 m). Hexagon backgrounds for labels indicate trace fossils, and circles indicate accessories (e.g., carbonaceous material, mud clasts). **A)** Hummocky cross stratified sandstone bed with mud clasts (mc) within Facies 1 mudstone. The laminated sandstone bed reveals the burrows (BI 2) present in Facies 1 (cross-section view, 211.5–215 m). **B)** Large, sand-filled *Thalassinoides* in Facies 1 mudstone (oblique view, 211.5–215 m). Trace fossil acronyms: *Palaeophycus* (Pa), *Rosselia* (Ro), *Teichichnus* (Te), and *Thalassinoides* (Th).

Teichichnus; and uncommon *Asterosoma, Conichnus, Cylindrichnus,* and *Schuabcylindrichnus* (Table 3). The ratio of shallow- to deep-tier trace

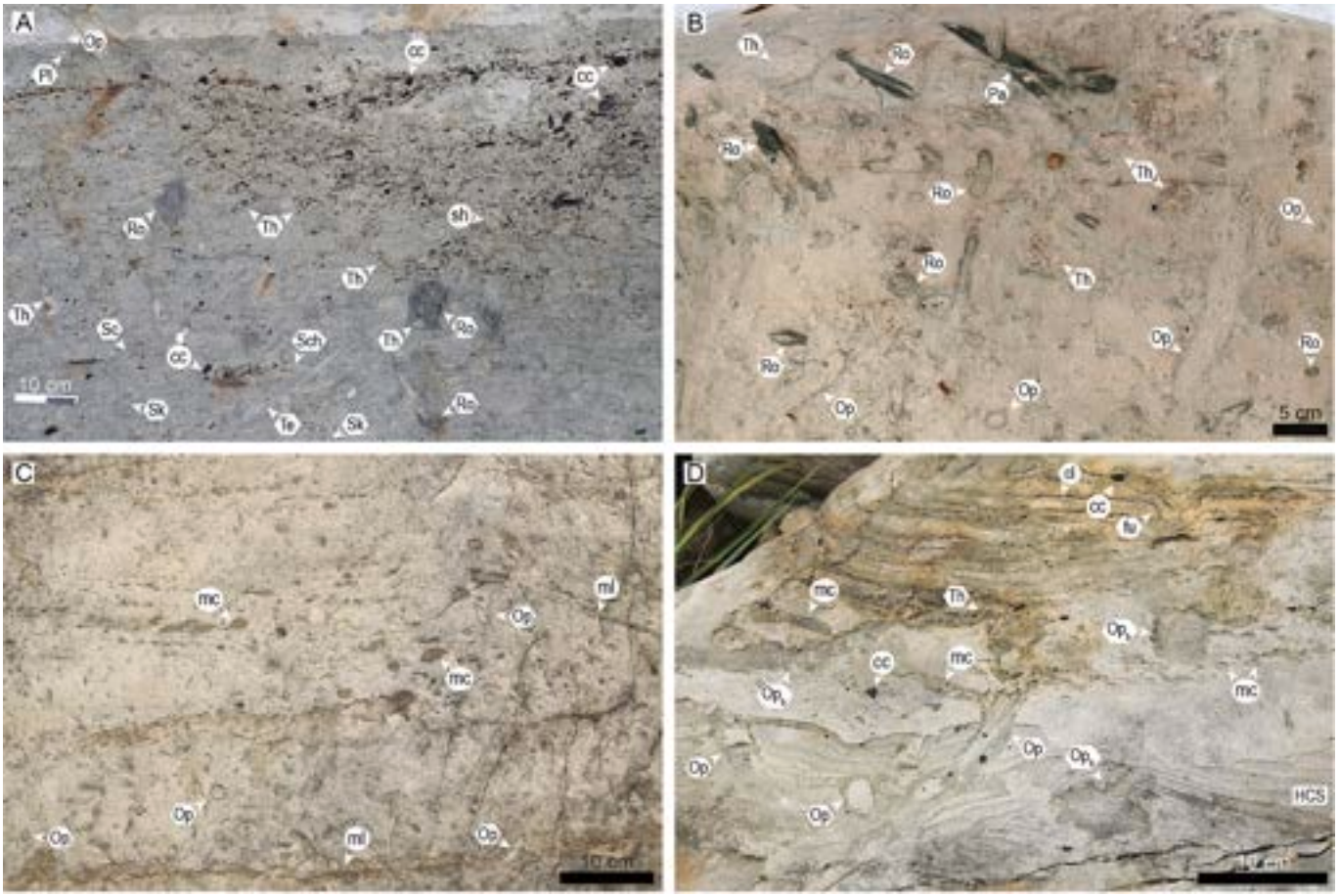

Fig. 7. Photos of the emergent–lower stage (239–340 m). Square backgrounds for labels indicate sedimentary structures, hexagons indicate trace fossils, and circles indicate accessories (e.g., carbonaceous material, mud clasts). **A)** A bed within Facies 2 of upper medium- to coarse-grained sandstone with coal clasts (cc) and shell fragments (sh) infilling *Thalassinoides*. Note the incorporation of coal clasts and shell hash into the highly bioturbated (BI 6) sandy mudstone that underlies the coarse-clastic layer (cross-section view, 245–248 m). **B)** Highly bioturbated (BI 6) sandstone of Facies 2 with coarse-clastic infilling of *Ophiomorpha, Palaeophycus*, *Rosselia*, and *Thalassinoides* (oblique view, 260.5–263 m). **C)** Hummocky cross-stratified sandstone (Facies 4) with mud lamina (ml) and mud clasts (mc). Bioturbation is low (BI 1–2) and the only visible burrow is *Ophiomorpha* (cross-section view, 290.5–294.5 m). **D)** Hummocky cross-stratified (HCS) sandstone (BI 2; Facies 4) with mud clasts overlain by parallel laminated sandstone (BI 1; Facies 3) with carbonaceous laminae (cl) and coal clasts (cc). Note the large, back-filled *Ophiomorpha* and collapsed laminae suggestive of fugichnia (oblique to cross-section view, 304.5–309.6 m). Trace fossil acronyms: back-filled *Ophiomorpha* (Op_b), fugichnia (fu), *Ophiomorpha* (Op), *Planolites* (Pl), *Rosselia* (Ro), *Schaubcylindrichnus* (Sch), *Scolicia* (Sc), *Skolithos* (Sk), *Teichichnus* (Te), and *Thalassinoides* (Th).

fossils is the highest of all stages (S:D = 4.4; Table 5). The most commonly observed trace fossils are associated with interface feeding followed by equal numbers of trace fossils that preserve filter feeding, deposit feeding, and other behaviours.

3.3. Emergent phase (239–571 m)

The emergent phase is divided into lower, middle, and upper stages. The division between the lower and middle stage is placed where strata of Facies 3 become more prevalent upwards (Fig. 3). The division between the middle and upper stage is placed where variability in both $\delta^{13}C_{org}$ values and facies increases upwards, with a corresponding decrease in the occurrence of Facies 2; this change is attributed to an intensification of tidal currents in the paleo-Taiwan Strait (Fig. 3).

The emergent–lower stage (239–340 m) comprises mainly Facies 2 and 4 (Figs. 3 and 7) with preservation of Facies 2 decreasing upwards. The trace fossil suite comprises 16 ichnogenera, including: abundant *Ophiomorpha*, *Rosselia*, and *Thalassinoides*; common *Palaeophycus*, *Phycosiphon*, *Planolites*, *Schaubcylindrichnus*, *Skolithos,* and *Teichichnus*; uncommon *Arenicolites, Asterosoma, Cylindrichnus, Piscichnus*, *Scolicia*, and *Siphonichnus*; and, rare *Conichnus* (Table 3). Variability in BI is bimodal in the emergent-lower stage with BI 5 and 6 preserved in 50% of the strata and BI 0–2 dominating in nearly 40% of strata (Table 4). The emergent–lower stage also preserves twice as many shallow-tier to deep-tier trace fossils (S:D = 2.2; Table 5). The trace fossil assemblage records a wide range of feeding behaviours with nearly equal traces recording deposit feeding, filter feeding and interface feeding.

The emergent–middle stage (340–407 m) comprises mainly Facies 3 and 4 (Figs. 3 and 8), with Facies 3 becoming increasingly common upwards. The trace fossil suite comprises 16 ichnogenera, including: abundant *Ophiomorpha*, *Planolites*, and *Thalassinoides;* common *Cylindrichnus, Helminthopsis, Palaeophycus*, *Rosselia*, and *Skolithos;* uncommon *Arenicolites, Conichnus, Macaronichnus, Phycosiphon*, *Piscichnus*, *Schaubcylindrichnus*, and *Scolicia* (Table 3). BI is notably lower in this stage, with >70% of the strata preserving BI 0–2 (Table 4). The emergent–middle stage preserves twice as many shallow-tier to deep-tier trace fossils (S:D = 2.2; Table 5), and the trace fossil assemblage records nearly equal numbers of deposit feeding and interface feeding ethologies followed closely by filter feeding.

The emergent-upper stage (407–571 m) comprises mainly Facies 3 and 4 (Table 1; Figs. 3 and 9). The trace fossil suite comprises 12 ichnogenera/ethological groups, including: abundant *Ophiomorpha*, *Planolites*, and *Thalassinoides*; common *Phycosiphon*, *Rosselia*, *Schaubcylindrichnus, Skolithos,* and *Teichichnus*; and, uncommon *Arenicolites, Chondrites*, *Diplocraterion,* and fugichnia (Table 3). Bioturbation is generally low throughout this stage with BI 0–2 preserved in >70% of all strata (Table 4). There is a notable decrease in the preservation of beds displaying BI 5 and 6 relative to the emergent-middle stage, and the ratio of shallow- to deep-tier trace fossils also decreases to 1.5 (Table 5). Trace fossils are mainly associated with deposit feeding followed by

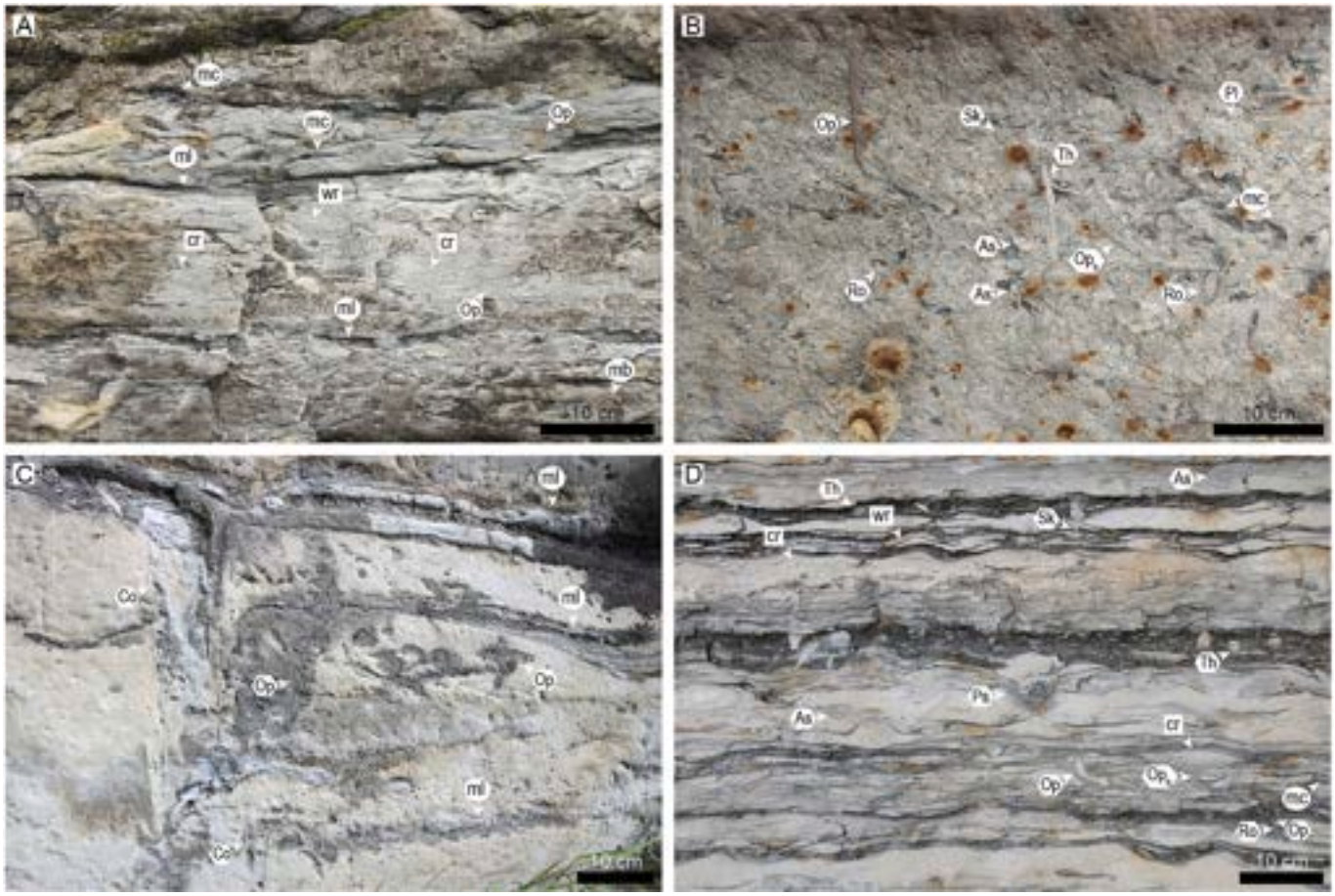

Fig. 8. Photos of the emergent–middle stage (340–407 m). **A)** Wavy-parallel laminated sandstone interbedded with current-ripple (cr) and wave-ripple (wr) laminated sandstone with mud clasts and laminated sandy mudstone (ml; Facies 3). Note the rare burrowing (BI 1) (cross-section view, 344.4–349.1 m). **B)** Completely bioturbated muddy sandstone (Facies 2) (cross-section view, 351.6–361.7 m). **C)** Large *Conichnus* and *Ophiomorpha* in interbedded trough cross-stratified to hummocky cross-stratified sandstone and wavy parallel laminated sandy mudstone (Facies 3) (cross-section view, 399 m). **D)** Interbedded flaser-bedded sandstone and wavy- to lenticular-bedded heterolithics (Facies 3) (cross-section view, 404 m). Trace fossil acronyms: *Asterosoma* (As), back-filled *Ophiomorpha* (Op_b), *Conichnus* (Co), *Ophiomorpha* (Op), *Planolites* (Pl), *Piscichnus* (Ps), *Rosselia* (Ro), *Skolithos* (Sk), and *Thalassinoides* (Th).

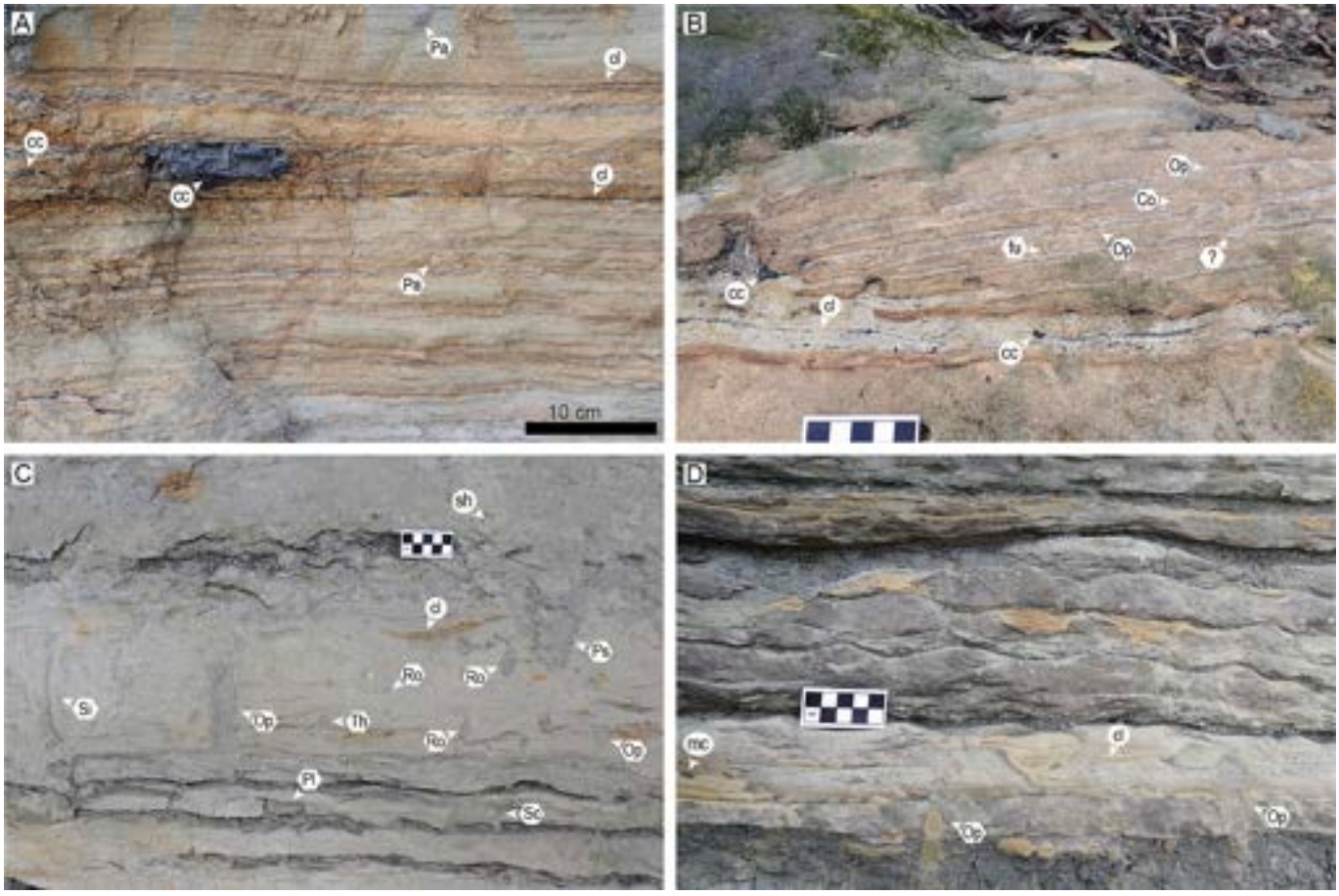

Fig. 9. Photos of the emergent–upper stage (407–571 m). Square backgrounds for labels indicate sedimentary structures, hexagons indicate trace fossils, and circles indicate accessories (e.g., carbonaceous material, mud clasts). All photos are shown in cross-section view and the black and white increments on the scale bars are in centimeters. **A)** Planar-parallel laminated sandstone within Facies 4 with carbonaceous laminae (cl) and coal clasts (cc). Bioturbation is minimal in this image (BI 1) (419–420 m). **B)** Low-angle planar-parallel laminated sandstone in Facies 3 with carbonaceous laminae and coal clasts. Bioturbation (BI 2) is highlighted by iron-cementation (459–460 m). **C)** Bioturbated muddy sandstone (BI 4) overlying wavy-bedded heterolithics (Facies 3, 536–537 m). **D)** Wavy-bedded heterolithics (BI 0) of Facies 3 with large *Ophiomorpha* in some beds (BI 2; 546–547 m). Trace fossil acronyms: *Conichnus* (Co), fugichnia (fu), *Ophiomorpha* (Op), *Palaeophycus* (Pa), *Piscichnus* (Ps), *Planolites* (Pl), *Rosselia* (Ro), *Scolicia* (Sc), *Siphonichnus* (Si), and *Thalassinoides* (Th).

filter feeding.

4. Discussion: ichnological trends through the emergence of Taiwan

Based on different phases of Taiwan's emergence and the development of the TWFB, the six stages defined in this study should reflect the changes from: 1) an open ocean setting (pre-emergent-lower), to 2) a semi-protected but fully subaqueous margin (pre-emergent-upper), to 3) a partly enclosed seaway on the landward side of an island that began receiving sediment through rapid erosion of poorly lithified and uplifted marine sediment (early emergent), to 4) a strait that received an overwhelming volume of sediment and organic material from emergent Taiwan but experienced limited tidal current amplification (emergent-lower), to 5) a strait in which tidal currents amplified and reworked seafloor sediment (emergent-middle), and finally, to 6) a strait that continued to receive nearly all its sediment and organic material from emergent Taiwan but also experienced increasingly strong tidal currents as the strait narrowed and elongated (emergent-upper)(Fig. 3; Dashtgard et al., 2021; Hsieh et al., 2023b; Hsieh et al., 2025). This six-part framework is used to interpret ichnological trends observed in the sedimentary strata (Tables 3–5; Fig. 10).

There are several distinct trends that can be observed in the trace fossil assemblages preserved in the Kueichulin Formation. First, the diversity and abundance of trace fossils, BI, and preservation of shallow-tier burrows in the pre-emergent-lower stage is substantially lower than in all overlying stages (Fig. 10). The preserved trace fossils also record predominantly deposit feeding. In the pre-emergent-lower stage, the uplifting but still submerged Taiwan probably provided little protection from sediment reworking by waves and currents generated during tropical cyclones travelling across the Pacific Ocean, and organic matter preserved in the studied section was derived mainly from marine sources (Fig. 3; Dashtgard et al., 2021; Hsieh et al., 2023b). Storm-related sediment reworking was intermittent; but was probably extensive as is suggested by the prevalence of mud-clast breccia and hummocky cross-stratification in these strata (Fig. 4; c.f.; Duke, 1985; Jelby et al., 2020; Snedden and Nummedal, 1991). The low intensity of bioturbation (>90% of strata display BI 0–1), and preservation of mainly deep-tier trace fossils (S:D = 0.3) support the interpretation of extensive hydraulic reworking of the uppermost bioturbated sediments below the seafloor, and hence, the limited preservation of shallow-tier burrows and bioturbated strata.

Second, the pre-emergent–upper and early emergent stages both show extensive bioturbation with 50–90% of beds displaying BI 4–6 (Table 5; Fig. 10B). There are corresponding major increases (relative to the pre-emergent-lower stage) in the diversity and density of abundant and commonly occurring ichnogenera (Table 3; Fig. 10A), in the preservation of structures attributed to filter feeding and interface feeding

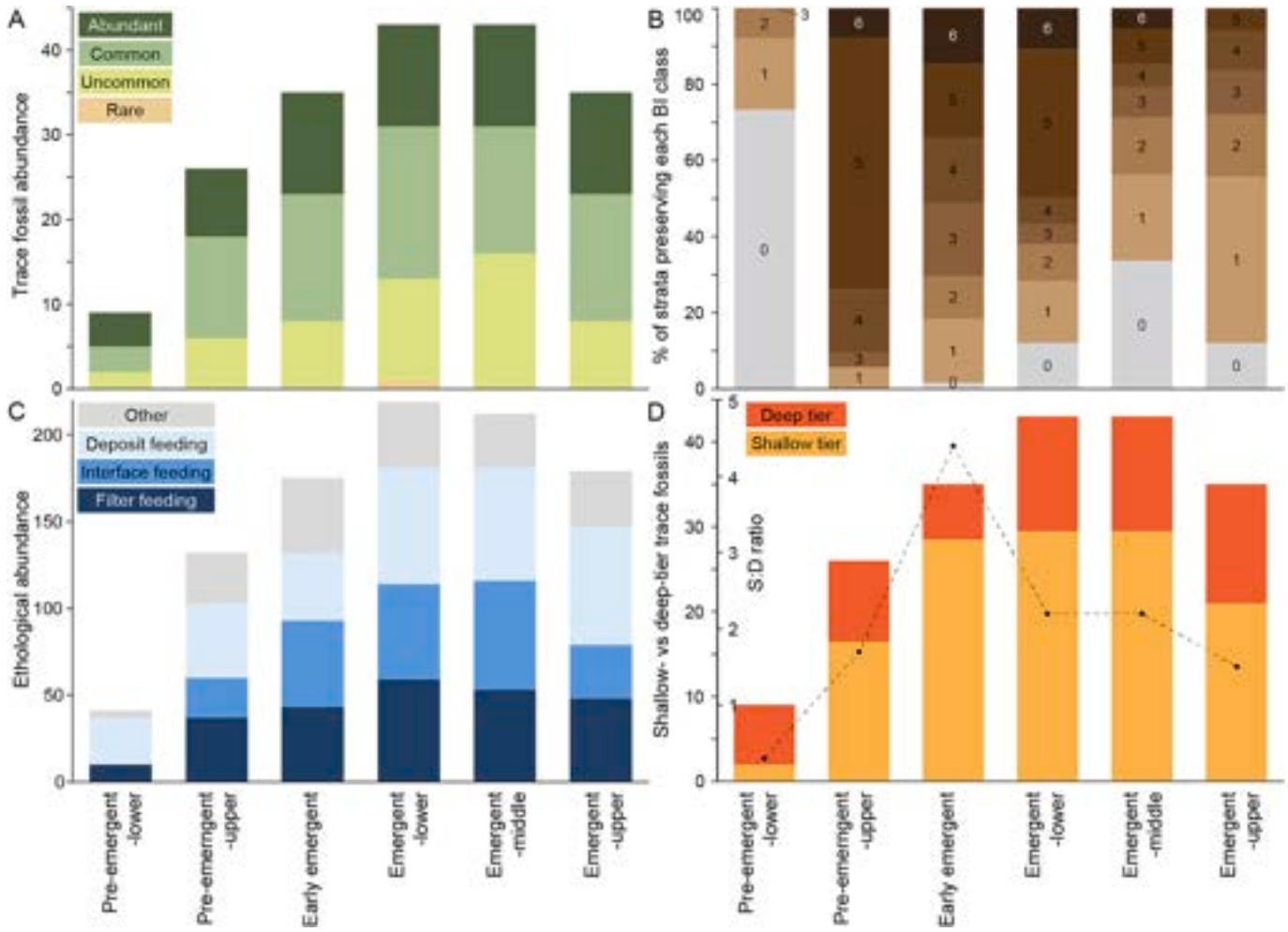

Fig. 10. Graphical expressions of ichnological data by stage. **A)** Ichnogenera abundance (Table 3). Values are calculated by multiplying the number of trace fossils in each category (e.g., abundant, common) by the value assigned to that category (e.g., abundant = 4). **B)** The net thickness of strata as a percentage of all strata in a stage that preserve different degrees of bioturbation as expressed by the Bioturbation Index (BI; Table 5). **C)** The prevalence of ichnogenera that represent the four groups of feeding modes and/or behaviours. Feeding modes and/or behaviours represented by trace fossils and their qualitative abundances are shown in Table 3 and semi-quantitative values are available in Table 4. **D)** The number of ichnogenera that are classified as either shallow tier or deep tier (Tables 3 and 4), and the shallow- to deep-tier ratio (S:D; black dots and dashed line). See Methods for an explanation of how values are derived.

(Table 4; Fig. 10C), and in the number of shallow-tier structures (Fig. 10D). The significant increase in all ichnological metrics from the pre-emergent-lower into the pre-emergent-upper stage correlates to Taiwan reaching a position below sea level where it probably served to baffle large waves from the Pacific Ocean and thus produced a relatively low-energy setting in the study area (leeward side of the orogen). This low-energy setting appears to have persisted from the pre-emergent-upper through emergent-middle stages. The reduction in sediment reworking by large waves is interpreted as the dominant control for the preservation of shallow-tier burrows.

Third, the density of bioturbation, diversity and abundance of individual ichnogenera, and preservation of shallow-tier trace fossils are highest through the emergent-lower and emergent-middle stages and then decline into the emergent-upper stage (Tables 3–5; Fig. 10). The decrease in trace fossil abundance and diversity from the emergent-middle to emergent-upper stages does not correspond to a decrease in trace fossils that occur regularly throughout the succession (i.e., common or abundant), but to a decrease in traces that are less commonly observed (i.e., uncommon and rare). As Taiwan propagated to the south and southwest (Nagel et al., 2013; Nagel et al., 2018), there would have been a corresponding lengthening and narrowing of the Taiwan Strait and amplification of currents passing through it. As well, the distance between proto-Taiwan and the study area would have decreased leading to increased sediment delivery to the study area and substrate mobility therein, especially during tropical cyclones (Dashtgard et al., 2020). Tropical cyclones in the Taiwan Strait would have been less intense than in the open Pacific Ocean but still preserve evidence of sediment erosion during storms. The combination of stronger currents, higher sediment loads, increased substrate mobility, and limited sediment erosion should be expressed in more variation and an overall decrease in the trace fossil density and diversity preserved in individual beds, and this appears to be the case (Fig. 10).

Finally, sediment lithology also plays a significant role in the preserved character of the trace fossil assemblage. Specifically, the mudstone-dominated early emergent phase/stage preserves considerably higher numbers of shallow-tier trace fossils compared to deep-tier trace fossils (Fig. 10C) and has the highest number of filter feeding and interface feeding structures relative to deposit feeding structures (2.4 vs 0.4–1.8 in the other stages). Variations in trace assemblages as a function of substrate has been reported in multiple neoichnological studies (e.g., Ayranci et al., 2014; Dashtgard et al., 2008; Gingras et al., 1999) and so it is expected. However, the shift towards mainly shallow-tier trace fossils and filter feeding and interface feeding over deposit feeding suggests that infauna do not preferentially burrow deeply in mud, probably in an attempt to avoid anoxic pore water or firm sediment at depth.

5. Conclusions

The Kueichulin Formation forms part of the fill of the Taiwan Western Foreland Basin and accumulated during the early stages of collision of the Luzon Arc on the Philippine Sea Plate with the Eurasian Plate and the associated uplift of the Taiwan Orogen. Consequently, the Kueichulin Formation records major shifts in basin geometry, sedimentation patterns and sources, and hydraulic conditions. Semi-quantitative characterization of the trace fossil assemblages preserved in the Kueichulin Formation are used to draw several conclusions:

1. Prior to emergence and during the early stages of emergence of Taiwan, the substantial increase in the density of bioturbation, diversity and abundance of ichnogenera, and preservation of shallow-tier structures is attributed to basin reconfiguration and Taiwan acting as a baffle to large storm waves generated across the Pacific Ocean during tropical cyclones. This buffering effect resulted in the increased preservation of shallow-tier burrows which include burrows attributed to filter feeders and interface deposit feeders.
2. With the emergence of the island and its south-southwestward propagation, narrowing and elongation of the Taiwan Strait resulted in the amplification of tidal currents and increased sediment delivery to the study area. Increased and more variable sedimentation / substrate mobility resulted in greater bed-by-bed variability in the degree of bioturbation. The amplification of tidal currents through the strait probably increased the delivery of suspended food particles and oxygenated water to the seafloor and this coincided with the introduction of significant quantities of terrestrial organic carbon (Fig. 3). The increased food and oxygenated water delivery is hypothesized to have driven the increase in the diversity of trace fossils recorded in emergent-lower and emergent-middle stages. However, continued amplification of tides and increasing sediment delivery to the study area is attributed with causing the reduction in all ichnological metrics from the emergent-middle to emergent-upper stages.
3. The integration of sedimentology and ichnology is fundamental to resolving depositional processes, and these interpretations are needed to determine the controls on the preservation of trace fossil assemblages. The association of sedimentary structures and bioturbation within and between beds demonstrate that sediment erosion, and especially seafloor erosion during storms, is the dominant control on the preservation and character of trace fossil assemblages through the Kueichulin Formation, and this concurs with previous studies (e.g., MacEachern and Pemberton, 1992; Pemberton et al., 2012).

The methodology employed herein demonstrates the value of a semi-quantitative approach to ichnology. While ichnological observations are and will remain qualitative in many respects, our approach depends on systematic, contextually informed logging that captures ichnological variability. The subsequent conversion of qualitative observations into semi-quantitative values can reveal subtle but significant trends in changing trace-fossil abundances, tiering depths, and ethologies, and thus provide a framework for assessing variable environmental and preservational controls on the character of trace-fossil assemblages.

CRediT authorship contribution statement

Shahin E. Dashtgard: Writing – review & editing, Writing – original draft, Visualization, Validation, Methodology, Investigation, Funding acquisition, Formal analysis, Data curation, Conceptualization. **Amy I. Hsieh:** Writing – review & editing, Visualization, Validation, Investigation, Formal analysis, Data curation. **Romain Vaucher:** Writing – review & editing, Visualization. **Ludvig Löwemark:** Writing – review & editing, Visualization, Methodology, Funding acquisition.

Declaration of competing interest

The authors declare no conflict of interest.

Acknowledgements

The authors thank the reviewers, Alina Shchepetkina and Luis Buatois, guest editors, Renata Netto and Noelia Carmona, and editor, Howard Falcon-Lang for their comments. We thank Yu-Yen Pan and Romy Setiaji for assistance in the field. This research was funded through a NSERC Discovery Grant to S.E. Dashtgard (RGPIN-2019-04528) and a NSTC grant (112–2116-M-002-018-MY3) to L. Löwemark. This work was also financially supported by the "The Featured Areas Research Center Program" within the framework of the Higher Education Sprout Project by the Ministry of Education in Taiwan.

Data availability

The authors confirm that all data necessary for supporting the scientific findings of this paper have been provided.

References

Ayranci, K., Dashtgard, S.E., MacEachern, J.A., 2014. A quantitative assessment of the neoichnology and biology of a delta front and prodelta, and implications for delta ichnology. Palaeogeogr. Palaeoclimatol. Palaeoecol. 409, 114–134.
Bromley, R.G., 1996. Trace Fossils: Biology, Taphonomy and Applications, 2nd edition. Chapman and Hall, London, UK.
Buatois, L.A., Gingras, M.K., MacEachern, J.A., Mángano, G.M., Zonneveld, J.-P., Pemberton, S.G., Netto, R.G., Martin, A., 2005. Colonization of brackish-water systems through time: evidence from the trace-fossil record. Palaios 20, 321–347.
Buatois, L.A., Mángano, M.G., Minter, N.J., Zhou, K., Wisshak, M., Wilson, M.A., Olea, R. A., 2020. Quantifying ecospace utilization and ecosystem engineering during the early Phanerozoic—the role of bioturbation and bioerosion. Sci. Adv. 6, eabb0618.
Castelltort, S., Nagel, S., Mouthereau, F., Lin, A.T., Wetzel, A., Kaus, B., Willett, S., Chiang, S.-P., Chiu, W.-Y., 2011. Sedimentology of early pliocene sandstones in the South-Western Taiwan foreland: Implications for basin physiography in the early stages of collision. J. Asian Earth Sci. 40, 52–71.
Chamberlain, C.K., 1978. Recognition of trace fossils in cores. In: Basan, P.B. (Ed.), Trace Fossil Concepts. SEPM (Society for Sedimentary Geology), pp. 119–166.
Chang, S.S.L., Chi, W.-R., 1983. Neogene nannoplankton biostratigraphy in Taiwan and the tectonic implications. Petrole. Geol. Taiwan 19, 93–147.
Chang, Q., Hren, M.T., Lai, L.S.-H., Dorsey, R.J., Byrne, T.B., 2023. Rapid topographic growth of the Taiwan orogen since ~1.3-1.5 ma. Sci. Adv. 9.
Chen, W.-S., Ridgway, K.D., Horng, C.-S., Chen, Y.-G., Shea, K.-S., Yeh, M.-G., 2001. Stratigraphic architecture, magnetostratigraphy, and incised-valley systems of the Pliocene-Pleistocene collisional marine foreland basin of Taiwan. Geol. Soc. Am. Bull. 113, 1249–1271.
Cohen, K.M., Gibbard, P.L., 2016. Global chronostratigraphical correlation table for the last 2.7 million years v. 2016a. In: QuaternaryChart1. International Commission on Stratigraphy. http://www.stratigraphy.org/index.php/ics-chart-timescale.
Cohen, K.M., Finney, S.C., Gibbard, P.L., Fan, J.-X., 2013. The ICS international chronostratigraphic chart. Episodes 36, 199–204.
Covey, M., 1984. Lithofacies analysis and basin reconstruction, Plio-Pleistocene western Taiwan foredeep. Petrole. Geol. Taiwan 20, 53–83.
Dashtgard, S.E., Gingras, M.K., 2012. Chapter 10: Marine Invertebrate Neoichnology. In: Knaust, D., Bromley, R.G. (Eds.), Trace Fossils as Indicators of Sedimentary Environments. Elsevier, pp. 273–295.
Dashtgard, S.E., Gingras, M.K., Pemberton, S.G., 2008. Grain-size controls on the occurrence of bioturbation. Palaeogeogr. Palaeoclimatol. Palaeoecol. 257, 224–243.
Dashtgard, S.E., Löwemark, L., Vaucher, R., Pan, Y., Pilarczyk, J., Castelltort, S., 2020. Tropical cyclone deposits in the pliocene Taiwan strait: processes, examples, and conceptual model. Sediment. Geol. 405.
Dashtgard, S.E., Löwemark, L., Wang, P.-L., Setiaji, R.A., Vaucher, R., 2021. Geochemical evidence of tropical cyclone controls on shallow-marine sedimentation (pliocene, Taiwan). Geology 49, 566–570.
Duke, W.L., 1985. Hummocky cross-stratification, tropical hurricanes, and intense winter storms. Sedimentology 32, 167–194.
Ekdale, A.A., Bromley, R.G., Knaust, D., 2012. The ichnofabric concept. In: Knaust, D., Bromley, R.G. (Eds.), Trace Fossils as Indicators of Sedimentary Environments. Elsevier, Amsterdam.
Gingras, M.K., Pemberton, S.G., Saunders, T., Clifton, H.E., 1999. The ichnology of modern and pleistocene brackish-water deposits at willapa bay, Washington: Variability in estuarine settings. Palaios 14, 352–374.
Gingras, M.K., Bann, K.L., MacEachern, J.A., Waldron, J., Pemberton, S.G., 2007. A conceptual framework for the application of trace fossils. In: MacEachern, J.A., Bann, K.L., Gingras, M.K., Pemberton, S.G. (Eds.), Applied Ichnology. SEPM (Society for Sedimentary Geology), Tulsa, USA, pp. 1–26.

Horng, C.-S., Shea, K.-S., 1996. Dating of the Plio-Pleistocene rapidly deposited sequence based on integrated magneto-biostratigraphy: a case study of the Madagida-Chi section, coastal range, eastern Taiwan. J. Geolog. Soc. China 39, 31–58.
Howard, J.D., Frey, R.W., 1984. Characteristic trace fossils in nearshore to offshore sequences, upper cretaceous of east-Central Utah. Can. J. Earth Sci. 21, 200–219.
Hsieh, A.I., Dashtgard, S.E., Clift, P.D., Lo, L., Vaucher, R., Löwemark, L., 2023a. Competing influence of the Taiwan orogen and East Asian summer monsoon on South China Sea paleoenvironmental proxy records. Palaeogeogr. Palaeoclimatol. Palaeoecol. 635, 111933.
Hsieh, A.I., Dashtgard, S.E., Wang, P.L., Horng, C.S., Su, C.C., Lin, A.T., Vaucher, R., Löwemark, L., 2023b. Multi-proxy evidence for rapidly shifting sediment sources to the Taiwan western foreland basin at the Miocene–Pliocene transition. Basin Res. 34, 932–948.
Hsieh, A.I., Vaucher, R., Löwemark, L., Dashtgard, S.E., Horng, C.S., Lin, A.T., Zeeden, C., 2023c. Influence of a rapidly uplifting orogen on the preservation of climate oscillations. Paleoceanography and Paleoclimatology 38.
Hsieh, A.I., Vaucher, R., MacEachern, J.A., Zeeden, C., Huang, C., Lin, A.T., Löwemark, L., Dashtgard, S.E., 2025. Resolving allogenic forcings on shallow-marine sedimentary archives of the Taiwan western foreland basin. Sedimentology 72, 1755–1785.
Jelby, M.E., Grudvåg, S.-A., Helland-Hansen, W., Olaussen, S., Stemmerik, L., 2020. Tempestite facies variability and storm-depostional processes across a wide ramp: Towards a polygenetic model for hummocky cross-stratification. Sedimentology 67, 742–781.
Kikuchi, K., Naruse, H., Kotake, N., 2018. Evaluation of ichnodiversity by Image-Resampling method to correct outcrop exposure bias. Palaios 33, 204–217.
La Croix, A.D., Ayranci, K., Dashtgard, S.E., 2022. Neoichnology of siliciclastic shallow-marine environments: Invertebrates, traces, and environmental conditions. Earth Sci. Rev. 233.
Lin, C.-W., Chen, W.-S., 2016. Geological Map of Taiwan. Geological Society of Taiwan, Taipei, Taiwan.
Lin, A.T., Watts, A.B., 2002. Origin of the West Taiwan basin by orogenic loading and flexure of a rifted continental margin. J. Geophys. Res. Solid Earth 107. ETG 2-1-ETG 2-19.
Lin, A.T.-S., Watts, A.B., Hesselbo, S.P., 2003. Cenozoic stratigraphy and subsidence history of the South China Sea margin in the Taiwan region. Basin Res. 15, 453–478.
Lin, A.T.-S., Wang, S.-M., Hung, J.-H., Wu, M.-S., Liu, C.-S., 2007. Lithostratigraphy of the Taiwan chelungpu-fault drilling project-a borehole and its neighboring region, Central Taiwan. Terr. Atmos. Ocean. Sci. 18.
MacEachern, J.A., Bann, K.L., 2020. The phycosiphon ichnofacies and the rosselia ichnofacies: two new ichnofacies for marine deltaic environments. J. Sediment. Res. 90, 855–886.
MacEachern, J.A., Pemberton, S.G., 1992. Ichnological aspects of cretaceous shoreface successions and shoreface variability in the Western Interior Seaway of North America. In: Pemberton, S.G. (Ed.), Applications of Ichnology to Petroleum Exploration, a Core Workshop. SEPM Society for Sedimentary Geology, Tulsa, pp. 57–84.
MacEachern, J.A., Bann, K.L., Pemberton, S.G., Gingras, M.K., 2007. The ichnofacies paradigm: High-resolution paleoenvironmental interpretation of the rock record. In: MacEachern, J.A., Bann, K.L., Gingras, M.K., Pemberton, S.G. (Eds.), Applied Ichnology. SEPM, Tulsa, USA, pp. 27–64.
Marenco, K.N., Hagadorn, J.W., 2019. Big bedding planes: Outcrop size and spatial heterogeneity influence trace fossil analyses. Palaeogeogr. Palaeoclimatol. Palaeoecol. 513, 14–24.
McIlroy, D., 2007. Lateral variability in shallow marine ichnofabrics: Implications for the ichnofabric analysis method. J. Geol. Soc. Lond. 164, 359–369.
MOEA, C.G.S.o.T, . Interactive Geological Map. http://gis.moeacgs.gov.tw/gwh/gsb97-1/sys8/index.cfm. Central Geological Survey, Taiwan.
Nagel, S., Castelltort, S., Wetzel, A., Willett, S.D., Mouthereau, F., Lin, A.T., 2013. Sedimentology and foreland basin paleogeography during Taiwan arc continent collision. J. Asian Earth Sci. 62, 180–204.
Nagel, S., Castelltort, S., Garzanti, E., Lin, A.T., Willett, S.D., Mouthereau, F., Limonta, M., Adatte, T., 2014. Provenance evolution during Arc-Continent collision: Sedimentary petrography of miocene to pleistocene sediments in the western foreland basin of Taiwan. J. Sediment. Res. 84, 513–528.
Nagel, S., Granjeon, D., Willett, S., Lin, A.T.-S., Castelltort, S., 2018. Stratigraphic modeling of the western Taiwan foreland basin: Sediment flux from a growing mountain range and tectonic implications. Mar. Pet. Geol. 96, 331–347.
Pan, T.-Y., Lin, A.T.-S., Chi, W.-R., 2015. Paleoenvironments of the evolving pliocene to early pleistocene foreland basin in northwestern Taiwan: an example from the dahan river section. Island Arc 24, 317–341.
Pemberton, S.G., MacEachern, J.A., 1997. Ichnological signature of storm deposits; the use of trace fossils in event stratigraphy. In: Brett, C.E., Baird, G.C. (Eds.), Paleontological Events; Stratigraphic, Ecological, and Evolutionary Implications. Columbia University Press, New York, USA, pp. 73–109.
Pemberton, S.G., MacEachern, J.A., Frey, R.W., 1992. Trace Fossil Facies Models: Environmental and Allostratigraphic Significance. In: Walker, R.G., James, N.P. (Eds.), Facies Models: Response to Sea Level Change. Geological Association of Canada, St. John's, Newfoundland, pp. 47–72.
Pemberton, S.G., MacEachern, J.A., Dashtgard, S.E., Bann, K.L., Gingrras, M.K., Zonneveld, J.-P., 2012. Chapter 19: Shorefaces. In: Knaust, D., Bromley, R.G. (Eds.), Trace Fossils as Indicators of Sedimentary Environments. Elsevier, pp. 563–603.
Reineck, H.-E., Singh, I.B., 1980. Depositional Sedimentary Environments, 2nd Ed. Springer-Verlag, Berlin.
Seike, K., Yanagishima, S., Nara, M., Sasaki, T., 2011. Large macaronichnus in modern shoreface sediments: Identification of the producer, the mode of formation, and paleoenvironmental implications. Palaeogeogr. Palaeoclimatol. Palaeoecol. 311, 224–229.
Seilacher, A., 1964. Biogenic Sedimentary Structures. In: Imbrie, J., Newell, N. (Eds.), Approaches to Paleoecology. Wiley, New York, pp. 296–316.
Seilacher, A., 1967. Bathymetry of trace fossils. Mar. Geol. 5, 413–428.
Shaw, C.-L., 1996. Stratigraphic correlation and isopach maps of the western Taiwan basin. Terr. Atmos. Ocean. Sci. 7, 333–360.
Shillito, A.P., Gougeon, R., 2024. Identifying and accounting for outcrop constraints on observations in field-based ichnological studies. Ichnos 30, 269–282.
Simoes, M., Avouac, J.P., 2006. Investigating the kinematics of mountain building in Taiwan from the spatiotemporal evolution of the foreland basin and western foothills. J. Geophys. Res. 111 (B10401), 1–25.
Singh, A., O'Regan, M., Coxall, H.K., Forwick, M., Lowemark, L., 2023. Exploring late pleistocene bioturbation on yermak plateau to assess sea-ice conditions and primary productivity through the ethological ichno quotient. Sci. Rep. 13, 17416.
Snedden, J.W., Nummedal, D., 1991. Origin and geometry of storm-deposited sand beds in modern sediments of the Texas continental shelf. In: Swift, D.J.P., Oertel, G.F., Tillman, R.W., Thorne, J.A. (Eds.), Shelf Sand and Sandstone Bodies: Geometry, Facies and Sequence Stratigraphy. International Association of SEdimentologists, London, pp. 283–308.
Suppe, J., 1981. Mechanics of mountain building and metamorphism in Taiwan. Memoi. Geological Society of China 4, 67–89.
Suppe, J., 1984. Kinematics of arc-continent collision, flipping of subduction and back-arc spreading near Taiwan. Memoi. Geological Society of China 6, 21–33.
Taylor, A.M., Goldring, R., 1993. Descriptions and analysis of bioturbation and ichnofabric. J. Geol. Soc. Lond. 150, 141–148.
Taylor, A., Goldring, R., Gowland, S., 2003. Analysis and application of ichnofabrics. Earth Sci. Rev. 60, 227–259.
Teng, L.S., Wang, Y., Tang, C.-H., Huang, C.-Y., Huang, T.-C., Yu, M.-S., Ke, A., 1991. Tectonic aspects of the paleogene depositional basin of northern Taiwan. Proceedings of the Geological Society of China 34, 313–336.
Vaucher, R., Dashtgard, S.E., Horng, C.-S., Zeeden, C., Dillinger, A., Pan, Y.-Y., Setiaji, R. A., Chi, W.-R., Löwemark, L., 2021. Insolation-paced Sea level and sediment flux during the early pleistocene in southeast asia. Sci. Rep. 11.
Vaucher, R., Dillinger, A., Hsieh, A.I., Chi, W.R., Löwemark, L., Dashtgard, S.E., 2023a. Storm-flood-dominated delta succession in the pleistocene Taiwan strait. Depositional Rec. 9, 820–843.
Vaucher, R., Zeeden, C., Hsieh, A.I., Kaboth-Bahr, S., Lin, A.T., Horng, C.-S., Dashtgard, S.E., 2023b. Hydroclimate dynamics during the Plio-Pleistocene transition in the northwest Pacific realm. Glob. Planet. Chang. 223.
Wang, Z., Miguez-Salas, O., 2025. Quantitative decoding of ediacaran locomotory trace fossil morphologies; evidence for the emergence of slender anterior-posterior body profiles. Geology 53, 732–736.
Wheatcroft, R.A., 1990. Preservation potential of sedimentary event layers. Geology 18, 843–845.
Yu, H.-S., Chou, Y.-W., 2001. Characteristics and development of the flexural forebuldge and basal unconformity of western Taiwan foreland basin. Tectonophysics 333, 277–291.
Zhang, L.J., Qi, Y.A., Buatois, L.A., Mangano, M.G., Meng, Y., Li, D., 2017. The impact of deep-tier burrow systems in sediment mixing and ecosystem engineering in early cambrian carbonate settings. Sci. Rep. 7, 45773.